THE ARGON-HYDROGEN EXPANDING THERMAL ARC PLASMA

R.F.G. Meulenbroeks, R.A.H. Engeln,
M.C.M. van de Sanden, J.A.M. van der Mullen, and D.C. Schram

Eindhoven University of Technology, Dept. of Physics
P.O.Box 513 5600 MB Eindhoven, The Netherlands

Abstract

An expanding thermal arc plasma that is used for deposition of thin films and as particle source is studied using active and passive spectroscopy. The argon-hydrogen plasma is characterized by very fast recombination, that cannot be explained by atomic processes. Thomson scattering, optical emission spectroscopy, and CARS measurements show, that the recombination is caused by molecular processes. Hydrogen molecules from the periphery of the expanding jet play a dominant role in the recombination process.

INTRODUCTION

Expanding thermal arc plasmas are used in a variety of applications, which include the deposition of diamond-like, amorphous carbon, and amorphous silicon thin films [1]. When the thermal arc is operated either on pure hydrogen or on an argon-hydrogen mixture, it could be used as a particle source for hydrogen radicals or hydrogen positive and negative ions [2,3]. Fundamental research on expanding plasmas focuses on the study of argon-hydrogen mixtures. The principle parameters that have to be determined are particle densities (electrons, neutrals and ions) and temperatures. To this end, active and passive spectroscopic techniques are employed. The results are interpreted by comparison with numerical models.

EXPERIMENT AND DIAGNOSTICS

The expanding thermal arc plasma is sketched in Fig. 1. The subatmospheric (0.2-0.6 bar) plasma is created in a cascaded arc, consisting of three cathodes, three electrically isolated copper plates, and an end anode plate. All the parts are water cooled. The diameter of the arc channel is 4 mm. The plasma is allowed to expand into a low pressure background through a conically shaped nozzle in the anode. The end of the nozzle (z=0) constitutes the beginning of the expansion in the z- direction.

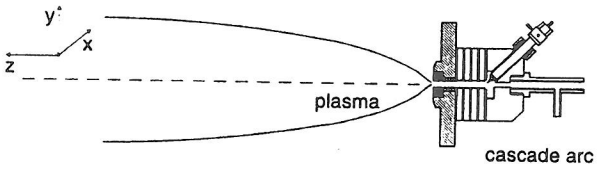

Figure 1: The expanding thermal arc plasma.

The hydrogen can be added to the plasma in two ways: either by burning the arc on a argon-hydrogen mixture, or by burning the arc on pure argon, and flushing hydrogen directly into the vessel. Standard conditions of the arc are: I=50 A, total flow: 3.5 SLM, background pressure 40-133 Pa.

The expanding plasma is characterized by a supersonic expansion ending in a stationary shock front (around z=40-70mm, depending on the background pressure) and followed by a subsonic relaxation region. In the expansion, where temperatures are around 2000 K, three particle recombination determines the ionization loss and the light emission, at least for the case of pure argon [4]. In the case of argon-hydrogen mixtures, important extra recombination channels are opened that involve hydrogen molecules [5].

Three diagnostics are applied to the plasma jet: *(1) Optical Emission Spectroscopy (OES)*: passive spectroscopy is used to determine the excited level populations of hydrogen and argon. The calibrated set up is described in [5]. *(2) Thomson-Rayleigh scattering*: a frequency doubled Nd:YAG laser is used for this diagnostic. Photons are scattered off free and bound electrons in the plasma and detection of the scattered (Doppler-shifted) radiation gives direct, local, and accurate information about electron and neutral densities and electron temperatures. The diagnostic has been described elsewhere [6]. *(3) Coherent Anti-Stokes Raman Scattering (CARS)*: in order to detect rovibrationally excited H_2, a CARS diagnostic has been realized.

CARS SPECTROSCOPY

The CARS process and signal generation has been described in a number of review articles (e.g., [7]) and we shall only give a brief account here. CARS is the coherent analogon of Raman scattering, with the advantage that the signal is created as a coherent beam, thus greatly enhancing the sensitivity.

The CARS signal (at frequency $\omega_3 = 2\omega_1 - \omega_2$) is generated through the third order non-linear susceptibility $\chi^{(3)}$ of the probed molecule. The anti-Stokes power (P_3) depends on the power of the pump (P_1 at ω_1) and Stokes (P_2 at ω_2) lasers as follows:

$$P_3 = K|\chi^{(3)}|^2 P_1^2 P_2, \tag{1}$$

where K is a proportionality constant. The $\chi^{(3)}$ consists of a resonant and a non-

resonant part: $\chi^{(3)} = \chi^{(3)}_{NR} + \chi^{(3)}_{res}$. The resonant part is greatly enhanced when a Raman resonance is probed, i.e., when $\omega_1 - \omega_2 = \omega_{v,J}$, where $\omega_{v,J}$ is the frequency of a particular Raman transition. The resonant part of $\chi^{(3)}$ is proportional to the difference in number densities between the probed states. Using a calibration on hydrogen gas and the measurement of a number of Raman resonances therefore yields absolute values of the population densities of individual rovibrational states. The effects of saturation by stimulated Raman scattering (SRS) were calculated using a code by M. Pealat *et al.* The laser powers were chosen in order to be in the region of very weak saturation [8].

The experiment is depicted in Fig. 2*a*. A Nd:YAG laser (Quanta Ray GCR230, 300mJ/pulse @ 532 nm, 50 Hz, single mode) is used for the ω_1 beam and to pump a Quanta Ray PDL3 dye laser (bandwidth around 0.07 cm^{-1}). The dye liquid is a mixture of DCM and LDS698 (Exciton) and delivers conversion in the region of 660-700 nm. The ω_1 and ω_2 beams are in a crossed beam arrangement (BOXCARS), and the detection volume has dimensions of about 30x0.3 mm. A small part (10%) of the beams is split off after the CARS lens (f=1 m) and led through a reference cell containing 7 bars of argon. The non-resonant signal created here is used as a reference to cancel out shot-to-shot variations in beam overlap and laser power, as well as variations in the dye laser output at different wavelengths. Both main and reference signals are detected using a 1 m monochromator (Mono1 and 2) and a fast phototube (PMT, Hamamatsu R1355). A fast, gated ADC integrates the PM tube outputs. The stepping of the dye laser and the monochromators, as well as the processing and storage of the ADC outputs is controlled by a PC.

RESULTS

The global properties of an expanding argon-hydrogen plasma become clear in Fig. 2*b*. The electron densities are depicted vs. the axial position z and the hydrogen content.

Two effects can be seen in Fig. 2*b*: (1) the electron density is lower right from the onset of the expansion when more hydrogen is added to the flow, and (2) at higher z-values, a very pronounced ionization loss is observed, which increases with increasing hydrogen content. The former effect is ascribed to a change in arc behaviour, whereas the latter observation must be due to some process of recirculation inside the vacuum vessel [5,9]. In this process, hydrogen atoms associate to molecules at the vessel walls and are transported towards the plasma beam again by reciculation. For lower hydrogen seed fractions, where the dominant ion is argon, the following reactions can occur:

$$Ar^+ + H_2 \longrightarrow ArH^+ + H, \tag{2}$$

$$ArH^+ + e \longrightarrow Ar + H^*, \tag{3}$$

during which excited H atoms are formed. The H_2 molecules necessary for these reactions originate from wall-association of H-atoms, supported by a strong recirculation

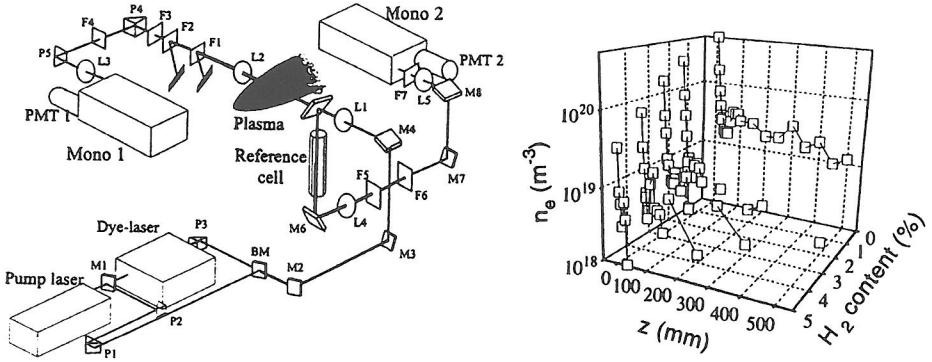

Figure 2: (*a*, left): the CARS spectrometer (*L*: lens, *M*: mirror, *BM*: dicroic mirror, *P*: prism, *F*: filter). (*b*, right): Thomson scattering results of the elctron density vs. the axial position and the hydrogen content. The arc burns on an argon-hydrogen mixture.

pattern in the vessel. A quasi one-dimensional model [9] solving mass, momentum and energy balances for the plasma particles confirms the existence of an external H_2 input into the jet. The model predicts, that this reentry flow penetrates the plasma around the shock position (i.e., around z=40-70 mm in Fig. 2*b*).

Absolute emission spectroscopy on the argon and hydrogen atomic systems shows, that all the argon emission disappears for seed fractions above 4-7 vol.%. As argon emission is due only to three particle recombination, this means that the arc does not produce any argon ions for this seed fractions. The dominant ion therefore probably is hydrogen for seed fractions above 7 vol.% [5,9]

To investigate more closely the reciculation effect a set of Thomson scattering experiments are performed: a comparison is made between a pure argon jet, a 2% hydrogen-in-argon jet and a pure argon jet with 2 vol.% hydrogen flushed directly into the vacuum vessel (Fig. 3*a*). The pure argon and "vessel injection" cases can be seen to clearly coincide completely up to z=100, i.e., the deviation starts after the shock region (this is in accordance with the model predictions). The hydrogen-argon "arc injection" case shows a similar behaviour, but has lower densities right from the start. The decrease after z=100 shows a remarkable symmetry between the "arc injection" and "vessel injection" cases. Eventually, a calculation shows, that equal amounts of molecular hydrogen are needed to explain the ionization loss after z=100. The ionization loss after the shock is thus thought to be totally determined by the background gas and the molecules present there.

The first aim of the CARS measurements was to scrutinize this phenomenon of anomalous recombination. CARS was performed on 10 and 50 vol. % H_2 in Ar mixtures (vessel and arc injection, I_{arc}=55 A, total flow 3.5 SLM, background

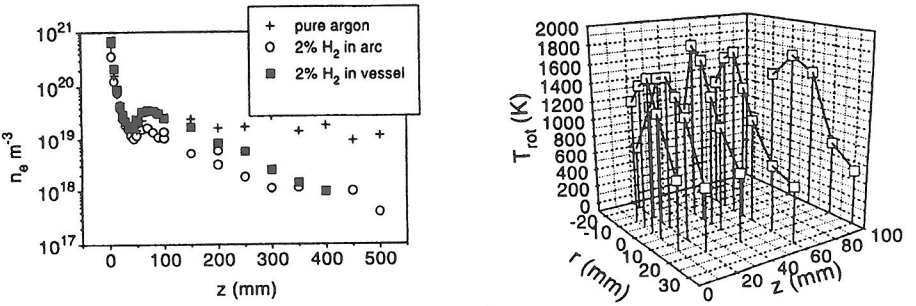

Figure 3: (*a*, left): Thomson scattering measurements on different types of expanding plasmas. (*b*, right): CARS measurements of the rotational temperature (v=1) in a 50 vol.% H_2 in Ar plasma (arc injection).

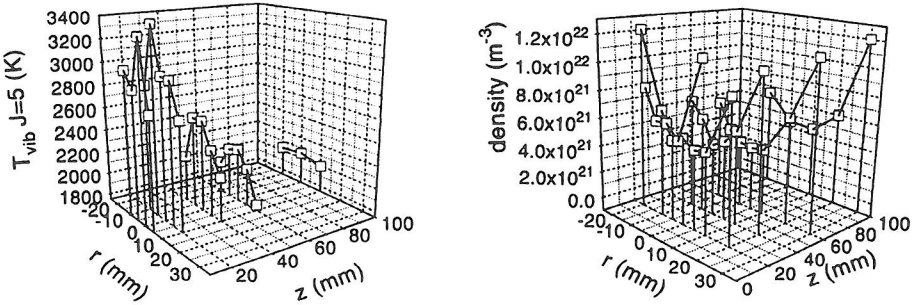

Figure 4: (*a*, left): CARS measurements of the vibrational temperature (J=5) in a 50 vol.% H_2 in Ar plasma (arc injection). (*b*, right): Total density profiles for this plasma.

pressure 133 Pa). In all cases, the view was confirmed, that the background gas contains primarily relatively cold (T_{rot}=400 K, T_{vib}=1000 K) hydrogen molecules. In fact, the relative partial hydrogen pressure in the periphery of the plasma appears to be equal to the seed fraction: a 10 vol. % seed fraction results in a partial hydrogen pressure that is equal to 10 % of the total background pressure. No highly excited vibrational states were detected within the detection limits (0.1 Pa at 300 K) in the periphery of the plasma.

The results of the measurements on a 50 vol.% H_2-Ar mixture are depicted in Figs. 3*b* and 4. Rotational temperatures are taken from the v=1 to v= 2 "hot band" Boltzmann plots. Vibrational temperatures are calculated comparing the J=5 populations in v=0 and v=1. In the calculation of the total absolute densities (Fig. 4*b*), the v=2 population is assumed to be negligible. The errors in the temperatures and

densities are estimated to be within 5-15%, depending on conditions.

Despite the very good sensitivity of the CARS spectrometer, no highly rovibrationally excited molecules are detected in the background gas. If any excitation is provided by wall association, it is lost by redistributing collisions before the molecules enter the plasma.

CONCLUSION

The expanding argon-hydrogen plasma jet is characterized by an anomalously fast recombination that can only be explained by molecular channels involving hydrogen molecules. For the recombination to be efficient in a plasma that is dominated by H^+, rovibrationally excited molecules are needed [3]. Active spectroscopy measurements show, that large amounts of hydrogen molecules are indeed present in the periphery of the plasma, even though they appear to be rather cool. A reciculation pattern in the vacuum vessel is thought to be responsible for the transport of (wall-associated) molecules into the plasma, most probably in the shock region.

ACKNOWLEDGEMENT

This work is supported by the Netherlands Technology Foundation (STW).

REFERENCES

/1/ A.J.M. Buuron, G.J. Meeusen, J.J. Beulens, M.C.M. van de Sanden, and D.C. Schram, J. Nucl. Mater. **200**, 430 (1993).
/2/ R.F.G. Meulenbroeks, D.C. Schram, L.J.M. Jaegers, and M.C.M. van de Sanden, Phys. Rev. Lett. **69** (9), 1379 (1992).
/3/ M.J. de Graaf, R. Severens, R.P. Dahiya, M.C.M. van de Sanden, and D.C. Schram, Phys. Rev. **E48** (3), 2098 (1993).
/4/ M.C.M. van de Sanden, J.M. de Regt, and D.C. Schram, Phys. Rev. **E47** (4), 2792 (1993).
/5/ R.F.G. Meulenbroeks, A.J. van Beek, A.J.G. van Helvoort, M.C.M. van de Sanden, and D.C. Schram, Phys. Rev. **E49** (5), 4397 (1994).
/6/ M.C.M. van de Sanden, J.M. de Regt, G.M. Janssen, J.A.M. van der Mullen, B. van der Sijde, and D.C. Schram, Rev. Sci. Instrum. **63**, 3369 (1992).
/7/ A.J. Druet and J.-P. E. Taran, Prog. Quant. Electron. **7**, 1 (1981).
/8/ M. Pealat, M. Lefebvre, B. Scherrer, *private communication*, M. Pealat, M. Lefebvre, and J.-P.E. Taran, Phys. Rev. **38** (4), 1948 (1988).
/9/ R.F.G. Meulenbroeks, R.A.H. Engeln, M.N.A. Beurskens, R.M.J. Paffen, M.C.M. van de Sanden, J.A.M. van der Mullen, and D.C. Schram, Plasma Sources Sci. Technol. **4**, 74 (1995).